
Stopping Bayesian Optimization with Probabilistic Regret Bounds

James T. Wilson

Abstract

Bayesian optimization is a popular framework for efficiently finding high-quality solutions to difficult problems based on limited prior information. As a rule, these algorithms operate by iteratively choosing what to try next until some predefined budget has been exhausted. We investigate replacing this de facto stopping rule with an (ϵ, δ) -criterion: *stop when a solution has been found whose value is within $\epsilon > 0$ of the optimum with probability at least $1 - \delta$ under the model*. Given access to the prior distribution of problems, we show how to verify this condition in practice using a limited number of draws from the posterior. For Gaussian process priors, we prove that Bayesian optimization with the proposed criterion stops in finite time and returns a point that satisfies the (ϵ, δ) -criterion under mild assumptions. These findings are accompanied by extensive empirical results which demonstrate the strengths and weaknesses of this approach.

1. Introduction

In the real world, we are often interested in finding a nearly optimal solution for a given problem. More specifically, we would like to find a solution that is sufficient for the task at hand (Simon, 1956). Many of these problems are not only expensive to solve but difficult to reason about without extensive background knowledge—such as discovering new chemicals (Griffiths & Hernández-Lobato, 2020), designing better experiments (von Kügelgen et al., 2019), or configuring machine learning algorithms (Snoek et al., 2012).

A common approach is therefore to construct models for these problem and use them to predict real-world outcomes. In recent years, Bayesian optimization (BO) has emerged as a leading approach for accomplishing these tasks. Precise definitions vary, but BO methods are frequently characterized by their use of probabilistic models to guide the search for good solutions. The idea is for these models

to provide predictive distributions over unknown results, which can then be used to simulate the usefulness of trying different things. These methods enjoy continued success on an increasingly diverse set of problems, many of which are beyond the scope of our presentation here. For a recent review of these topics, see Garnett (2023).

Despite these successes, an ongoing issue for practitioners has been the persistent lack of user-friendly stopping rules. The vast majority of BO runs proceed until a predetermined budget (usually, a number of trials or amount of resources) has been exhausted. While there are many reasons for this trend, the primary cause is likely mistrust in the underlying model. After all, if the model is bad then the algorithm is liable to stop much too soon or far too late. To avoid potential disappointment, let us say upfront that this criticism is valid and will not be resolved in this work. We will return to this point when discussing experiments in Section 6.

At the same time, there are many applications where models have repeatedly proved to be reliable. Especially in these settings, there is much to be gained by using models to help us decide when to stop. One benefit of model-based stopping is its ability to adapt to the data. Sometimes we will get lucky and stumble upon a good solution early on. Other times, we will struggle to make progress. If the model accounts for these events, then stopping decisions can be tailored to reflect the peculiarities of individual runs.

Another benefit of model-based stopping is that it can simplify the user experience by allowing us to better communicate our goals. Choosing a budget is fairly unintuitive. Unless one has dealt with many similar problems before, it can be difficult to gauge the amount of resources to allocate for search. One of our aims is therefore to express stopping conditions in a language that is easier to understand. To this end, we focus on the case where the user deems a solution sufficient if its value is within $\epsilon > 0$ of the best possible outcome with probability at least $1 - \delta$. We show how this goal can be accomplished in a principled and practical way.

The remaining text is organized as follows. Section 2 reviews background material. Section 3 presents the idea behind our approach. Section 4 uses this premise to construct a practical algorithm. Section 5 analyzes this algorithm’s properties when the true model is known. Finally, Section 6 examines performance under ideal and realistic conditions.

Correspondence to: <j.wilson17@imperial.ac.uk>.

Preliminary work. Under review by the International Conference on Machine Learning (ICML).

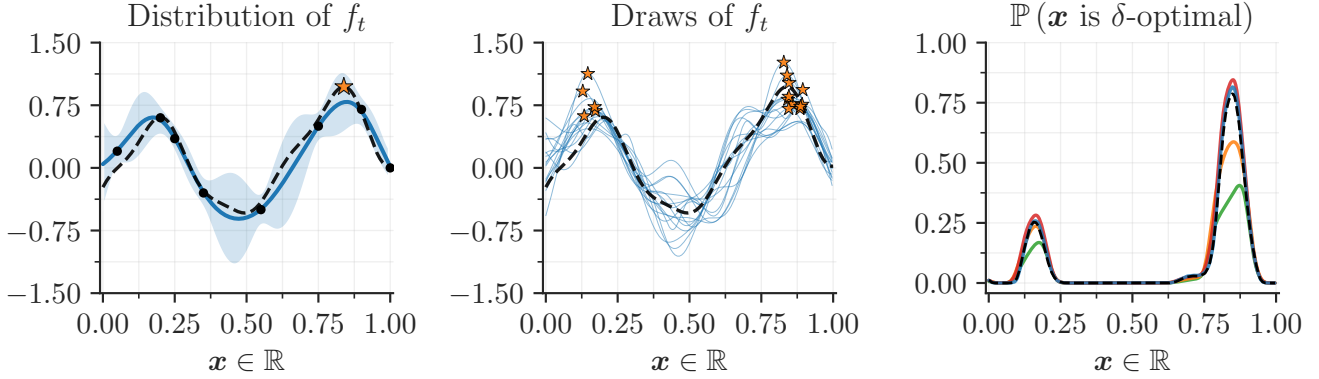


Figure 1. *Left*: Posterior mean and two standard (blue) given 8 observations (black dots) of $y(\cdot) \sim \mathcal{N}(f(\cdot), 10^{-2})$. The goal is to find an $\mathbf{x} \in \mathcal{X}$ whose true function (dashed black line) value is within $\epsilon > 0$ of the optimum (orange star). *Middle*: Draws of $f_t \sim \mathcal{GP}(\mu_t, k_t)$ are shown in blue alongside corresponding samples of f_t^* (orange stars). *Right*: Various approximations for (4) under the given posterior. Ground truth (dashed black) was established by assessing (6) with location-scale-based samples of f_t on a dense grid. All other methods simulated f_t using the approximate sampling method from Wilson et al. (2020). The resulting approximation to (6) is portrayed in blue. The remaining methods analytically integrated out $f_t(\mathbf{x})$, while potentially conditioning on f_t^* . $\mathbb{P}(r_t(\mathbf{x}) \geq \epsilon)$ is shown in orange, $\mathbb{P}(r_t(\mathbf{x}) \geq \epsilon \mid f_t(\mathbf{x}) \leq f_t^*)$ in green, and $\mathbb{P}(r_t(\mathbf{x}) \geq \epsilon \mid f_t(\mathbf{x}) \leq f_t^*, f_t(\mathbf{x}^*) = f_t^*)$ in red where $\mathbf{x}^* \in \arg \min_{\mathbf{x} \in \mathcal{X}} f_t(\mathbf{x})$ is sampled.

2. Background

We will use lowercase and uppercase boldface characters to denote vectors and matrices, respectively. By minor abuse of notation, we will write, e.g., $\mathbf{X}_n = \{\mathbf{x}_i : i = 1, \dots, n\}$ for a set consisting of $n \in \mathbb{N}$ items, typically the first n elements of a sequence (\mathbf{x}_n) . For a function $h : \mathcal{X} \rightarrow \mathbb{R}$, we will similarly write $h(\mathbf{X}_n) = \{h(\mathbf{x}_i) : i = 1, \dots, n\}$ and sometimes treat this set as an n -dimensional vector.

The left panel of Figure 1 portrays a prototypical problem, the details of which are expanded upon below. We are given a function $f : \mathcal{X} \rightarrow \mathbb{R}$ and tasked with finding a point $\mathbf{x} \in \mathcal{X}$ whose value is within $\epsilon > 0$ of the optimum $f^* = \sup_{\mathbf{x} \in \mathcal{X}} f(\mathbf{x})$. Such a point will be said to be ϵ -optimal.

At time $t \in \mathbb{N}$, our understanding of f will be based on prior knowledge and any data that we have collected so far. We will therefore use a model to help us make informed decisions. Different types of models are eligible and methods introduced below will only require the ability to simulate whether points are ϵ -optimal. We focus on the most popular model family in this setting: Gaussian processes (GPs).

A Gaussian process is a random function $f : \mathcal{X} \times \Omega \rightarrow \mathbb{R}$ with the property that, for any finite subset $\mathbf{X} \subseteq \mathcal{X}$, the random variable $f(\mathbf{X}) : \Omega \rightarrow \mathbb{R}^{|\mathbf{X}|}$ is Gaussian in distribution. We will write $f \sim \mathcal{GP}(0, k)$ for a centered GP with covariance function $k : \mathcal{X} \times \mathcal{X} \rightarrow \mathbb{R}$. We model the observed outcomes of trials $\mathbf{X}_t \in \mathcal{X}^t$ as function values corrupted by independent Gaussian noise and denote them by $y(\mathbf{X}_t) \sim \mathcal{N}(f(\mathbf{X}_t), \gamma^2 \mathbf{I})$. Given $y(\mathbf{X}_t)$, our understanding of f is represented by the posterior process

$f_t \sim \mathcal{GP}(\mu_t, k_t)$, where $\mathbf{\Lambda} = k(\mathbf{X}_t, \mathbf{X}_t) + \gamma^2 \mathbf{I}$ defines

$$\mu_t(\mathbf{x}) = k(\mathbf{x}, \mathbf{X}_t) \mathbf{\Lambda}^{-1} y(\mathbf{X}_t) \quad (1)$$

$$k_t(\mathbf{x}, \mathbf{x}') = k(\mathbf{x}, \mathbf{x}') - k(\mathbf{x}, \mathbf{X}_t) \mathbf{\Lambda}^{-1} k(\mathbf{X}_t, \mathbf{x}'). \quad (2)$$

An example of a GP posterior can be seen in Figure 1.

Throughout, we assume that \mathcal{X} is compact and that μ_t and k_t are both continuous so that they attain their limits on \mathcal{X} . Among other things, this assumption allows us to write $\mathbf{s}_t \in \arg \max_{\mathbf{x} \in \mathbf{S}_t} \mu_t(\mathbf{x})$ for a preferred solution at time t , where \mathbf{S}_t is either the set of queried points \mathbf{X}_t or space \mathcal{X} .

3. Premise

In practice, we will rarely ever know if a point $\mathbf{x} \in \mathcal{X}$ is truly ϵ -optimal. Instead, we must rely upon a model to provide an educated guess. If this model is probabilistic, then we would like to know its view on the probability that \mathbf{x} is ϵ -optimal. More formally, define the *regret* incurred by a solution $\mathbf{x} \in \mathcal{X}$ under the model at time t as

$$r_t(\mathbf{x}) = f_t^* - f_t(\mathbf{x}), \quad (3)$$

where $f_t^* = \sup_{\mathbf{x} \in \mathcal{X}} f_t(\mathbf{x})$ is the best predicted outcome. The model-based probability of \mathbf{x} being ϵ -optima is then¹

$$\Psi_t(\mathbf{x}; \epsilon) = \mathbb{P}(r_t(\mathbf{x}) \leq \epsilon). \quad (4)$$

We propose to search for better solutions until we have found a point that satisfies a *probabilistic regret bound*

$$\text{PRB}_t(\mathbf{x}; \epsilon, \delta) = \begin{cases} 1 & \Psi_t(\mathbf{x}; \epsilon) \geq 1 - \delta \\ 0 & \text{otherwise,} \end{cases} \quad (5)$$

¹We will often omit ϵ as an argument of Ψ_t to ease notation.

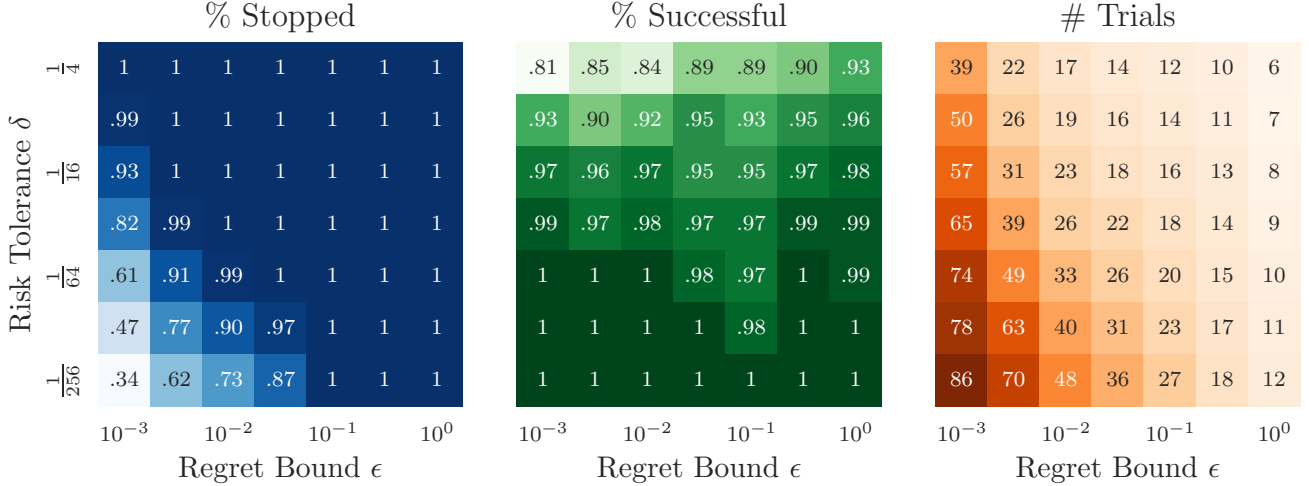


Figure 2. Simulated stopping behavior using PRB when $f : [0, 1]^2 \rightarrow \mathbb{R}$ is drawn from a known prior with noise variance $\gamma^2 = 10^{-4}$. Regret bounds $\epsilon > 0$ control how close $f(\mathbf{x})$ must be to the optimal value f^* for the point $\mathbf{x} \in \mathcal{X}$ to be deemed satisfactory. Risk tolerances $\delta > 0$ upper bound the probability that the returned point fails to be ϵ -optimal. *Left*: Percent of runs that stopped before time $T = 128$. *Middle*: Percent of stopped runs that returned ϵ -optimal points. *Right*: Median number of trials performed by stopped runs.

where *risk tolerance* $\delta > 0$ upper bounds the probability that we fail to return an ϵ -optimal solution. Points that meet this requirement will be said to be (ϵ, δ) -optimal.

As a rule, the ϵ -optimality probability (4) is intractable. We therefore assume that samples of f_t^* and $f_t(\mathbf{x})$ will be used to generate a Monte Carlo estimate

$$\Psi_t^n(\mathbf{x}; \epsilon) = \frac{1}{n} \sum_{i=1}^n \mathbb{1}(r_t^i(\mathbf{x}) \leq \epsilon), \quad (6)$$

where $r_t^i(\mathbf{x})$ is the i -th draw of the model-based regret (3). Figure 1 illustrates this procedure by visualizing draws of f_t and comparing different approximations to (4).

We now would like to use Ψ_t^n to test (5). While $\Psi_t^n(\mathbf{x}) \geq 1 - \delta$ does not guarantee that $\Psi_t(\mathbf{x}) \geq 1 - \delta$, we may bound the estimation error inherent to $\Psi_t^n(\mathbf{x})$ with high probability and use this bound to infer whether the latter event is likely to hold. We accomplish this task with the help of the following inequality from Audibert et al. (2007), a variant of which was also studied by Maurer & Pontil (2009),

Theorem 1 (Empirical Bernstein bound). *Let X_1, \dots, X_n be independent and identically distributed copies of a random variable $X \in [a, b]$ with empirical mean and variance*

$$\bar{X}_n = \frac{1}{n} \sum_{i=1}^n X_i \quad \bar{\sigma}_n^2 = \frac{1}{n} \sum_{i=1}^n (X_i - \bar{X}_n)^2. \quad (7)$$

It follows with probability at least $1 - \delta$ that

$$|\bar{X}_n - \mathbb{E}[X]| \leq \Delta_n, \quad (8)$$

where $\Delta_n = \bar{\sigma}_n \sqrt{\frac{2 \log(3/\delta)}{n}} + \frac{3(b-a) \log(3/\delta)}{n}$.

This bound was chosen because it decays faster than, e.g., Hoeffding’s inequality when the sample variance is significantly smaller than the sample range. We are interested in inferring whether an event occurs with high probability, so this variance will vanish as the true probability goes to one.

In order to test the criterion (5), choose any nonzero probabilities δ_{mod} and δ_{est} so that $(1 - \delta_{\text{mod}})(1 - \delta_{\text{est}}) \geq 1 - \delta$. As we will see shortly, $\lambda = 1 - \delta_{\text{mod}}$ lower bounds the chance that \mathbf{x} is ϵ -optimal under the model $\Psi_t(\mathbf{x}) = \mathbb{E}[X]$. Meanwhile, $1 - \delta_{\text{est}}$ lower bounds the probability that we correctly infer whether $\Psi_t(\mathbf{x}) \geq \lambda$ based on a draw of $\Psi_t^n(\mathbf{x}) = \bar{X}_n$. The rationale for this inference is explained below and previously appeared in Bardenet et al. (2014).

Suppose we draw $\Psi_t^n(\mathbf{x})$. If this draw is closer to $\Psi_t(\mathbf{x})$ than it is to the decision boundary λ , then $\Psi_t^n(\mathbf{x})$ and $\Psi_t(\mathbf{x})$ must be positioned on the same side of λ . Consequently, we would be able to tell if $\Psi_t(\mathbf{x}) \geq \lambda$ by looking at $\Psi_t^n(\mathbf{x})$. According to Theorem 1, the distance $|\Psi_t^n(\mathbf{x}) - \Psi_t(\mathbf{x})|$ vanishes as $n \rightarrow \infty$ with high probability. For now, assume we have chosen $n \in \mathbb{N}$ in such a way that

$$|\Psi_t^n(\mathbf{x}) - \Psi_t(\mathbf{x})| < |\Psi_t^n(\mathbf{x}) - \lambda| \quad (9)$$

holds in at least $1 - \delta_{\text{est}}$ percent of cases.² Then, $\Psi_t^n(\mathbf{x}) \geq \lambda$ implies the probability that \mathbf{x} is ϵ -optimal is greater than or equal to $(1 - \delta_{\text{mod}})(1 - \delta_{\text{est}}) \geq 1 - \delta$.

This line of reasoning is the basic premise of our method. We will generate enough draws of f_t so that our estimate is likely closer to $\Psi_t(\mathbf{x})$ than it is to λ . We will then use this estimate to decide whether or not $\Psi_t(\mathbf{x}) \geq \lambda$.

²We may assume that $\Psi_t(\mathbf{x}) \neq \lambda$ with probability one. Note that $\Psi_t(\mathbf{x})$ is only random prior to making the first t observations.

Figure 2 illustrates how PRB behaves for different regret bounds ϵ and risk tolerances δ . Data was generated by running BO a hundred times and jointly sampling f_t^* and $f_t(\mathbf{s}_t)$ a thousand times at steps $t = 5, \dots, 127$. These samples were used to evaluate $\Psi_t^n(\mathbf{s}_t, \epsilon)$ and stopping was simulated by comparing these estimates with $\lambda = 1 - \delta_{\text{mod}}$, where $\delta_{\text{mod}} = \frac{\delta}{2}$. As ϵ and δ go to zero, PRB becomes increasingly strict and stopping times are seen to increase. Encouragingly, the success rates of stopped runs are consistently close to or in excess of $1 - \delta$. The same is not true when estimates are directly compared to $1 - \delta$, since this does not account for estimation errors. Note that $n = 1000$ samples is often not enough to ensure correct decisions are made with high probability when $|\Psi_t^n(\mathbf{s}_t, \epsilon) - \lambda|$ is small.

A remaining question is how to choose sample sizes $n \in \mathbb{N}$. In practice, drawing f_t^* can often be fairly expensive. Our immediate goal is therefore to design an algorithm that allows us to avoid paying for a gratuitous number of samples.

4. Method

This section shows how to convert the preceding ideas into practical algorithms. At each time $t \in \mathbb{N}$, we will use a Monte Carlo estimate (6) to test the PRB criterion. The number of samples used to construct these estimates will be chosen online by Algorithm 1 (discussed below) such that each estimate may be used to confidently infer whether a point is ϵ -optimal. We review this algorithm first and then give details on how, when, and where to test PRB.

Algorithm 1 operates by drawing i.i.d. copies of a random variable X until a bound on the resulting estimation error is sufficiently tight for it to confidently decide whether or not $\mathbb{E}[X] \geq \lambda$. To better understand this, start by defining a pair of sequences: sample sizes (n_j) and risk tolerances (δ_j) . The sizes should be increasing, while the tolerances should be positive and satisfy $\sum_{j=1}^{\infty} \delta_j \leq \delta$.

For every $j \in \mathbb{N}$, use the first n_j copies of X to define an event that holds with probability at least $1 - \delta_j$

$$\mathcal{E}_j = \{|\bar{X}_{n_j} - \mathbb{E}[X]| \leq \Delta_{n_j}\}, \quad (10)$$

where Δ_{n_j} is the confidence bound given in Theorem 1. Each event corresponds to a simple test: if \mathcal{E}_j obtains and $|\bar{X}_{n_j} - \lambda| \geq \Delta_{n_j}$, \bar{X}_{n_j} is on the same side of λ as $\mathbb{E}[X]$. Suppose we generate draws of X until we encounter the first $j \in \mathbb{N}$ such that $|\bar{X}_{n_j} - \lambda| > \Delta_{n_j}$ and use this estimate to determine if we think that $\mathbb{E}[X] \geq \lambda$. By definition of (δ_j) and the union bound, we have

$$\mathbb{P}(\mathcal{E}_1, \dots, \mathcal{E}_j) \geq 1 - \sum_{i=1}^j \mathbb{P}(\mathcal{E}_i^c) \geq 1 - \delta. \quad (11)$$

Hence, our decision is correct with probability at least $1 - \delta$.

Algorithm 1 Adaptive Empirical Bernstein Classifier

- 1: Given a random variable $X : \Omega \rightarrow [a, b]$, a boundary $\lambda \in [a, b]$, an increasing sequence of natural numbers (n_j) , and a positive sequence (δ_j) s.t. $\sum_{j=1}^{\infty} \delta_j \leq \delta$.
 - 2: Initialize $j = 0, n = 0, \bar{\mu} = 0, \bar{\nu} = 0$, and $\Delta = \infty$.
 - 3: **while** $|\bar{\mu} - \lambda| < \Delta$ **do**
 - 4: $j \leftarrow j + 1$
 - 5: $\mathbf{x} \leftarrow [X(\omega_{n+1}), \dots, X(\omega_{n+j})]^\top$ // Get $n_j - n$ draws
 - 6: $\mathbf{y} \leftarrow \mathbf{x} - \bar{\mu}$
 - 7: $n \leftarrow n_j$
 - 8: $\bar{\mu} \leftarrow \bar{\mu} + n^{-1} \mathbf{1}^\top \mathbf{y}$ // Update mean
 - 9: $\bar{\nu} \leftarrow \bar{\nu} + (\mathbf{x} - \bar{\mu})^\top \mathbf{y}$ // Update squared error
 - 10: $\Delta \leftarrow n^{-1} \left(\sqrt{2 \log(3/\delta_j)} \bar{\nu} + 3(b-a) \log(3/\delta_j) \right)$
 - 11: **end while**
 - 12: Return $\mathbb{1}(\bar{\mu} \geq \lambda)$ // $\mathbb{P}[\mathbb{1}(\bar{\mu} \geq \lambda) \neq \mathbb{1}(\mathbb{E}[X] \geq \lambda)] \leq \delta$
-

This algorithm is not new. Algorithm 1 was inspired by Mnih et al. (2008) and references contained therein, who studied how concentration inequalities like Theorem 1 can be used to iteratively test for convergence in the sense that $\mathbb{P}(|\bar{X}_n - \mathbb{E}[X]| \leq \epsilon \mathbb{E}[X]) \geq 1 - \delta$. As mentioned earlier however, our approach is closer to Bardenet et al. (2014). There, a variant of Algorithm 1 was used to decide whether or not to accept Metropolis-Hastings proposals based on subsampled log likelihood estimates. This application is quite different from ours, but the underlying task of inferring whether an expected value exceeds a level is the same.

We follow Mnih et al. (2008) by setting $\delta_j = j^{-\alpha} \frac{(\alpha-1)}{\alpha} \delta$ where $\alpha = 1.1$. Given an initial sample size $n_0 \in \mathbb{N}$, we similarly define $n_j = \lceil \beta^{j-1} n_0 \rceil$ where $\beta = 1.5$. We set $n_0 = 64$ when estimating Ψ_t . Using a geometric schedule for (n_j) helps to avoid cases where δ_j shrinks unnecessarily due to a large number of tests being performed with a small number of samples. In exchange, this schedule can result in nearly β times too many samples being drawn.

Figure 3 shows how Algorithm 1 behaves when deciding whether $\mathbb{E}[X] \geq \lambda$, where $X \sim \text{Bern}(p)$. As $p \rightarrow 1$, the distance between \bar{X}_n and λ tends to increase and a decision can be made with larger confidence bounds constructed using fewer draws of X . As $\delta \rightarrow 1$, these bounds decrease and a decision can similarly be made using fewer samples.

4.1. How to sample $X = \mathbb{1}(r_t(\mathbf{x}) \leq \epsilon)$

We propose to sample f_t via pathwise conditioning (Wilson et al., 2020; 2021). More specifically, we suggest to approximate the prior with a Bayesian linear model

$$\hat{f}(\cdot) = \phi(\cdot)^\top \mathbf{w} \quad \mathbf{w} \sim \mathcal{N}(\mathbf{0}, \mathbf{I}), \quad (12)$$

where the feature map $\phi : \mathcal{X} \rightarrow \mathbb{R}^\ell$ is randomly generated so that $\phi(\mathbf{x})^\top \phi(\mathbf{x}') \approx k(\mathbf{x}, \mathbf{x}')$ (Rahimi & Recht, 2007).

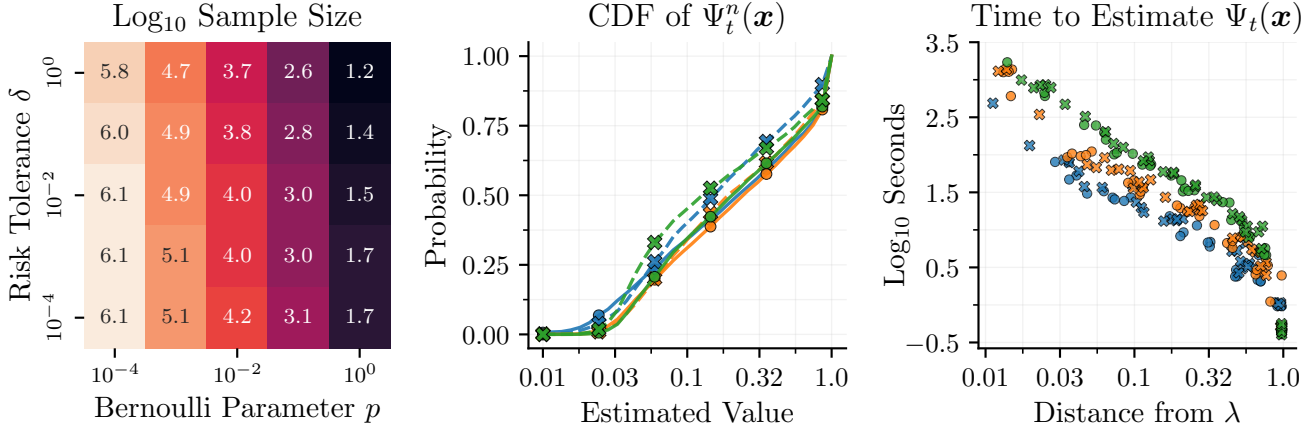


Figure 3. *Left*: Median number of draws used by Algorithm 1 to decide if the expectation of a Bernoulli random variable $X \sim \text{Bern}(p)$ exceeds $\lambda = 10^{-5}$ (chosen arbitrarily). *Middle*: Empirical CDFs of Ψ_t^n when running BO with known priors $\mathcal{GP}(0, k)$ in two, four, and six dimensions given noise variance $\gamma^2 = 10^{-6}$ (solid, \circ) or $\gamma^2 = 10^{-2}$ (dashed, \times). Here, $\epsilon = 0.1$ and $\delta_{\text{mod}} = \delta_{\text{est}} = 0.025$. *Right*: Runtimes of Algorithm 1 using the sampling procedure described in Section 4 and an approximate time limit of one thousand seconds.

Denoting $\Lambda = k(\mathbf{X}_t, \mathbf{X}_t) + \gamma^2 \mathbf{I}$ and $\varepsilon \sim \mathcal{N}(\mathbf{0}, \gamma^2 \mathbf{I})$, we may then use Matheron’s rule to approximate draws from the posteriors as

$$f_t(\cdot) \stackrel{d}{\approx} \hat{f}(\cdot) + k(\cdot, \mathbf{X}_t) \Lambda^{-1} [\mathbf{y}_t - \hat{f}(\mathbf{X}_t) - \varepsilon]. \quad (13)$$

Given a draw of f_t , indicators $\mathbb{1}(r_t(\mathbf{x}) \leq \epsilon)$ can then be obtained using multi-start gradient ascent. A helpful insight is that generating indicators with function draws eliminates the need to find f_t^* . For each draw of f_t , it suffices to determine if there exists a point $\mathbf{x}' \in \mathcal{X}$ such that $f_t(\mathbf{x}') - f_t(\mathbf{x}) > \epsilon$. This property can be exploited to speed up the process of sampling $\mathbb{1}(r_t(\mathbf{x}) \leq \epsilon)$, however these benefits typically fall off as $\Psi_t(\mathbf{x})$ increases.

It should be said that this sampling procedure introduces a yet-to-be-determined amount of error in practice, since draws of f_t are not only approximate but non-convex. Initial results suggest these errors are small (see Figure 1), however we leave this as a topic for future investigation.

Figure 3 reports empirical distributions for $\Psi_t^n(s_t)$ and wall times for Algorithm 1 under the given sampling procedure. Runtimes were found to primarily depended on the distance from $\Psi_t^n(s_t)$ to λ and dimensionality of $\mathcal{X} = [0, 1]^D$. The latter trend largely occurred because the number of starting positions we considered was exponential in D . Overall, it is clear that letting Algorithm 1 pick sample sizes $n \in \mathbb{N}$ leads to substantial savings over using a large static value.

4.2. When and where to test for ϵ -optimality

At each step $t \in \mathbb{N}$ (or a subsequence thereof), we will use Algorithm 1 to infer $(\epsilon, \delta_{\text{mod}})$ -optimality with accepted risk less than or equal to $\delta_{\text{est}}^t > 0$. Defining $\sum_{t=1}^{\infty} \delta_{\text{est}}^t \leq \delta_{\text{est}}$ allows us to (union) bound the probability that any test

fails and, hence, that BO stops prematurely.

When testing multiple points per step, we must therefore divide δ_{est}^t in order to retain this bound. Draws of f_t can be shared, but decreasing δ_{est}^t may cause the algorithm to request additional samples (see Figure 3). Results from the next section suggest it suffices to test s_t , but this practice may lead to suboptimal stopping times. If solutions are restricted to \mathbf{X}_t , then we may safely ignore any $\mathbf{x} \in \mathbf{X}_t$ for which $\mathbb{P}(f_t(s_t) - f_t(\mathbf{x}) \geq \epsilon) \geq \delta_{\text{mod}}$. In practice, we found that this heuristic usually eliminates most candidates.

More generally, we may use gradient information to maximize an estimator for Ψ_t based on one of the (approximate) conditioning strategies from Figure 1. The resulting points can then be tested with an independent run of Algorithm 1 (independent in the sense that draws of f_t are not recycled).

5. Analysis

We will show that Bayesian optimization with the PRB stopping criterion not only terminates, but does so correctly with high probability. We begin by discussing the assumptions made throughout this section:

- A1. The search space $\mathcal{X} = [0, 1]^D$ is a unit hypercube.
- A2. $f \sim \mathcal{GP}(0, k)$, where $k : \mathcal{X} \times \mathcal{X} \rightarrow \mathbb{R}$ is a known covariance function with Lipschitz constant L_k , i.e. $|k(\mathbf{x}, \mathbf{x}) - k(\mathbf{x}, \mathbf{x}')| \leq L_k \|\mathbf{x} - \mathbf{x}'\|_{\infty}$ for all $\mathbf{x}, \mathbf{x}' \in \mathcal{X}$.
- A3. The sequence (\mathbf{x}_t) is almost surely dense in \mathcal{X} .

A1 and A2 guarantee it is possible for the maximum posterior variance to become arbitrarily small based on a finite number of observations. A3 then implies that this event will almost surely occur in finite time. More generally, A3

is necessary to ensure convergence when the only things we know are that \mathcal{X} is compact and f is continuous (Törn & Žilinskas, 1989).

When A1 and A2 hold, certain strategies are known to produce almost surely dense iterates. For instance, Vazquez & Bect (2010) showed that Expected Improvement (Šaltenis, 1971), Probability of Improvement (Kushner, 1962), and Knowledge Gradient (Moćkus, 1975; Frazier et al., 2009) all exhibit this behavior when f is observed. This condition can also be enforced by introducing a small chance that \mathbf{x}_t will be chosen at random (Sutton & Barto, 2018).

We first prove that Bayesian optimization satisfies the PRB criterion with probability one when solutions may be freely chosen on \mathcal{X} . An extension of this result for cases where solutions are restricted to \mathbf{X}_t is given in Appendix A.

Theorem 2. *Under assumptions A1–A3 and for all regret bounds $\epsilon > 0$ and risk tolerances $\delta > 0$, there almost surely exists a $T \in \mathbb{N}$ so that, at every time $t \geq T$, each point $\mathbf{s}_t \in \arg \max_{\mathbf{x} \in \mathcal{X}} \mu_t(\mathbf{x})$ satisfies*

$$\mathbb{P} \left[\sup_{\mathbf{x} \in \mathcal{X}} f_t(\mathbf{x}) - f_t(\mathbf{s}_t) \leq \epsilon \right] \geq 1 - \delta. \quad (14)$$

Proof. See Appendix A. \square

To understand the proof of Theorem 2, consider the process

$$g_t(\cdot) = \underbrace{f_t(\cdot) - f_t(\mathbf{s}_t)}_{\text{performance gap}} + \underbrace{\mu_t(\mathbf{s}_t) - \mu_t(\cdot)}_{\geq 0}. \quad (15)$$

By construction, g_t is centered and its supremum satisfies

$$g_t^* = \sup_{\mathbf{x} \in \mathcal{X}} g_t(\mathbf{x}) \geq \sup_{\mathbf{x} \in \mathcal{X}} f_t(\mathbf{x}) - f_t(\mathbf{s}_t) = r_t(\mathbf{s}_t). \quad (16)$$

Hence, it suffices to upper bound the probability that g_t^* is greater-equal to ϵ . Such a bound may be obtain using the Borell-TIS inequality (Borell, 1975; Tsirelson et al., 1976)

$$\mathbb{P}(g_t^* \geq \epsilon) \leq \exp \left(-\frac{1}{2} \left[\frac{\epsilon - \mathbb{E}(g_t^*)}{2\sigma_t} \right]^2 \right) \quad (17)$$

which holds $\forall \epsilon > \mathbb{E}(g_t^*)$, where $\sigma_t^2 = \max_{\mathbf{x} \in \mathcal{X}} k_t(\mathbf{x}, \mathbf{x})$. In (17), we divide by $2\sigma_t$ since $\max_{\mathbf{x} \in \mathcal{X}} \text{Var}[g_t(\mathbf{x})] \leq 4\sigma_t^2$. From here, one can prove that $\mathbb{E}(g_t^*)$ decreases as $\sigma_t \rightarrow 0$. The remaining task is therefore to show that σ_t becomes arbitrarily small as \mathbf{X}_t becomes increasingly dense in \mathcal{X} .

Similar ideas can be found in Grünewälder et al. (2010), who proved that the expected regret goes to zero under like assumptions. These authors showed that BO will converge; we show that we will know it has done so. Equipped with this knowledge, we now demonstrate that the algorithm stops successfully with high probability.

Theorem 3. *Given a regret bound $\epsilon > 0$ and risk tolerance $\delta > 0$, let $\Psi_t(\mathbf{s}_t)$ be the probability under the model at time $t \in \mathbb{N}$ that $\mathbf{s}_t \in \arg \max_{\mathbf{x} \in \mathcal{X}} \mu_t(\mathbf{x})$ is ϵ -optimal. Suppose that at each step t (or a subsequence thereof) an independent run of Algorithm 1 is used to produce a random, unbiased estimate $\Psi_t^n(\mathbf{s}_t)$ that is closer to $\Psi_t(\mathbf{s}_t)$ than it is to $1 - \delta_{\text{mod}}$ with probability at least $1 - \delta_{\text{est}}^t$, where δ_{mod} and δ_{est} are nonzero probabilities so that $\delta_{\text{mod}} + \delta_{\text{est}} \leq \delta$ and (δ_{est}^t) is a positive sequence satisfying $\sum_{i=1}^{\infty} \delta_{\text{est}}^i \leq \delta_{\text{est}}$.*

If assumptions A1–A3 hold and the first \mathbf{s}_t for which $\Psi_t^n(\mathbf{s}_t) \geq 1 - \delta_{\text{mod}}$ is returned, then the algorithm almost surely finishes in finite time with an (ϵ, δ) -optimal solution.

Proof. See Appendix A. \square

The proof of Theorem 3 is straightforward. Since A1–A3 hold and estimates to $\Psi_t(\mathbf{s}_t)$ at each step are independent and unbiased, Theorem 2 implies there almost surely exists a first time $T \in \mathbb{N}$ where $\Psi_T(\mathbf{s}_T) \geq \lambda$ and $\Psi_T^n(\mathbf{s}_T) \geq \lambda$. The probability of terminating prior to this point is at most $\sum_{t=1}^{T-1} \delta_{\text{est}}^t \leq \delta_{\text{est}}$ by the union bound, and the probability that \mathbf{s}_T fails to be ϵ -optimal is at most δ_{mod} . As a result, the algorithm stops and returns a solution that is ϵ -optimal with probability at least $1 - \delta_{\text{mod}} - \delta_{\text{est}} \geq 1 - \delta$.

Let us now see how well this theory holds up in practice.

6. Experiments

Experiments discussed here were performed by first running BO with conservatively chosen budgets $T \in \mathbb{N}$. We then stepped through each saved run with different stopping rules to establish stopping times and terminal performance. This paradigm ensured fair comparisons and reduced overheads. For each problem, a hundred independent runs of BO were used to generate the reported results. Note that despite the general notation of the paper, all problems were defined as minimization tasks. Full details can be found in Appendix B and extended results are presented in Appendix C. Code is available online at https://github.com/j-wilson/trieste_stopping.

For PRB, we divided δ evenly between δ_{est} and δ_{mod} . Since experiments were carried out using preexisting BO runs that each began with five random trials and ended at times T , we employed a constant schedule $\delta_{\text{est}}^t = \frac{1}{T-5} \delta_{\text{est}}$ for the accepted amount of risk at steps $t \in \mathbb{N}$. Parameter schedules for Algorithm 1 are described in Section 4.

As a practical concession, we limited each run of Algorithm 1 to 1000 draws of f_t and used the resulting estimate to decide whether to stop—even if the corresponding bound was not sufficiently tight to provide guarantees. Preliminary results under this setup were consistent with those discussed in Figure 3, so we opted to limit the number of sam-

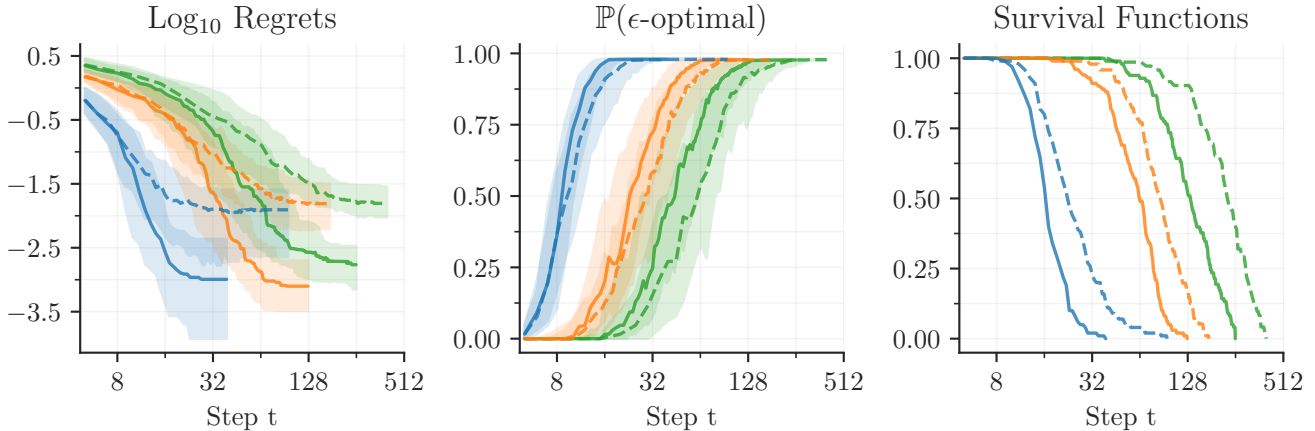


Figure 4. Results on functions drawn from known priors $\mathcal{GP}(0, k)$ in two, four, and six dimensions with noise variance $\gamma^2 = 10^{-6}$ (solid) or $\gamma^2 = 10^{-2}$ (dashed). *Left*: Medians and interquartile ranges of log regrets $\log_{10}[\sup_{\mathbf{x} \in \mathcal{X}} f(\mathbf{x}) - f(\cdot)]$. *Middle*: Medians and interquartile ranges of estimated ϵ -optimality probabilities $\max_{\mathbf{x} \in \mathbf{X}_t} \Psi_t^n(\mathbf{x})$. *Right*: Empirical probabilities of evaluating t or more trials. In the first two panels, sequences were padded with their final values to accommodate different lengths.

ples in order to run more experiments on a wider range of problems. Additionally, when optimizing $f \sim \mathcal{GP}(0, k)$ in six dimensions with noise $\gamma^2 = 10^{-2}$, we evaluated PRB once every five steps to further expedite these experiments.

Baselines We tested several baselines, many of which we granted access to information that is usually unavailable (indicated by an asterisk). We summarize these as follows:

- M1.** Oracle*: stops once an ϵ -optimal point is observed.
- M2.** Budget: stops after a predetermined number of trials.
- M3.** Budget*: same as above, but with limits retroactively set to the smallest values such that at least $1 - \delta$ percent of runs returned ϵ -optimal results (where possible).
- M4.** Acquisition cutoff: stops once the acquisition value of the next trial falls below a given threshold.
- M5.** UCB – LCB: stops when the gap between upper and lower confidence bounds is less than or equal to ϵ , i.e.

$$\max_{\mathbf{x} \in \mathcal{X}} \text{UCB}_t(\mathbf{x}) - \max_{\mathbf{x}' \in \mathbf{X}_t} \text{LCB}_t(\mathbf{x}') \leq \epsilon,$$

where $[\text{U/L}]CB_t(\mathbf{x}) = \mu_t(\mathbf{x}) \pm \sqrt{\beta_t k_t(\mathbf{x}, \mathbf{x})}$.

M1 is the optimal stopping rule, but requires perfect information for f . Similarly, M3 is the optimal fixed budget in hindsight. For M2, we allocated $16D$ trials per experiment in order to balance simplicity and performance.

M4 is discussed by Jones (2001), Nguyen et al. (2017), and references contained therein for Expected Improvement, which is closely related to the 1-step optimal strategy used in our experiments. We stopped when acquisition values

fell below a threshold of 10^{-5} , chosen post-hoc by walking powers of ten and selecting the best performing value.

Lastly, M5 was proposed by (Makarova et al., 2022). This method could seemingly provide guarantees akin to those discussed in Section 5. However, the suggested schedule $\beta_t = \frac{2}{5} \log(Dt^2\pi^2/6\delta)$ does not afford such a promise.³

Below, we discuss results when optimizing draws from known priors $f \sim \mathcal{GP}(0, k)$ and then proceed to the case where models were fit online to the observed data.

6.1. Results with known models

Figure 4 shows how PRB runs evolved over time. Median stopping times increased with dimensionality D and noise variance γ^2 . While not evident in this plot, ϵ -optimality probabilities $\max_{\mathbf{x} \in \mathbf{X}_t} \Psi_t^n(\mathbf{x})$ tended to increase over time and occasionally dip back down when encountering better-than-expected outcomes that caused the model to reconsider how f behaves on different regions of \mathcal{X} .

The top half of Table 1 summarizes the stopping times and success rates of each method on synthetic problems. Here, PRB compared favorably and either outperformed or kept pace with all (non-oracle) baselines. As was true for the simulations presented in Section 3, PRB success rates were consistently close to or above the 95% target rate.

M3 and M4 performed well in our experiments—save for on Branin, where M4 often reached the limit of $T = 64$ trials. This performance can largely be explained for by the fact that we used their optimal parameter values. It is unclear how these value should be set in practice. We found

³Srinivas et al. (2009, Lemma 5.1) uses a union bound over \mathcal{X} , so β_t usually depends on cardinality $|\mathcal{X}|$ not dimensionality D .

Stopping Bayesian Optimization with Probabilistic Regret Bounds

	GP-2*, 10 ⁻⁶	GP-2*, 10 ⁻²	GP-4*, 10 ⁻⁶	GP-4*, 10 ⁻²	GP-6*, 10 ⁻⁶	GP-6*, 10 ⁻²
Oracle*	10 (100%)	11 (100%)	27 (100%)	29.5 (100%)	40.5 (99%)	65 (100%)
Budget*	18 (96%)	23 (96%)	65 (95%)	95 (95%)	125 (95%)	228 (96%)
Budget	33 (98%)	33 (100%)	65 (95%)	65 (85%)	97 (86%)	97 (70%)
Acq. Cutoff*	26 (99%)	60.5 (100%)	76.5 (100%)	89 (96%)	115.5 (97%)	145 (92%)
UCB – LCB	12 (89%)	82 (100%)	22.5 (66%)	256 (100%)	32.5 (50%)	512 (100%)
PRB (ours)	17 (97%)	23 (99%)	64 (99%)	86.5 (96%)	133.5 (98%)	235 (100%)

	GP-4, 10 ⁻⁶	GP-4, 10 ⁻²	Branin-2	Hartmann-3	Hartmann-6	Rosenbrock-4
Oracle*	35 (100%)	51 (100%)	19 (100%)	14 (100%)	36 (67%)	34 (100%)
Budget*	80 (95%)	158 (95%)	26 (95%)	23 (96%)	256 (67%)	47 (95%)
Budget	65 (85%)	65 (61%)	33 (100%)	49 (100%)	97 (67%)	65 (100%)
Acq. Cutoff*	77.5 (97%)	112 (96%)	64 (100%)	25 (100%)	38 (67%)	62 (94%)
UCB – LCB	18 (30%)	224 (80%)	31 (99%)	15 (83%)	26 (46%)	73.5 (100%)
PRB (ours)	61 (88%)	100.5 (92%)	33 (99%)	19 (100%)	40 (64%)	84 (100%)

Table 1. Median stopping times and success rates when seeking (ϵ, δ) -optimal solutions, where $\delta = 0.05$ and $\epsilon = 0.1$. For Rosenbrock, $\epsilon = 10^{-4}$. Numbers atop each column denote the dimensionality of $\mathcal{X} = [0, 1]^D$ followed by the noise variance γ^2 (where present). Asterisks indicate that information which would normally be unavailable was used to set parameters to their optimal values. Non-oracle methods that returned ϵ -optimal solutions at least $1 - \delta$ percent of the time using the fewest function evaluations are shown in blue.

that M5 struggled to terminate in the presence of moderate noise. This tendency can be understood by comparing the various estimators in Figure 1. Decoupling f_t^* and $f_t(\mathbf{s}_t)$ causes excess competition between $f_t(\mathbf{s}_t)$ and positively correlated process values (including itself).

We also observe that the gap between PRB and oracle stopping times often grew much faster than oracle stopping times themselves did. This pattern emerges because we only need to learn about f at an appropriately chosen point to find an ϵ -optimal solution. In contrast, we must learn about f globally to verify ϵ -optimality. This interpretation agrees with empirical analysis in which we found that PRB stopping times correlated more with how function values concentrated around f^* than with the first time at which an ϵ -optimal point was observed. We speculate that strategies which better account for the goal of finding an (ϵ, δ) -optimal point may help to bridge this gap. Similar ideas were previously explored by Cai et al. (2021).

6.2. Results with maximum likelihood models

Results for this setting occupy the bottom half of Table 1. As seen in Appendix C, BO performance was consistently strong. However, this performance did not always translate to the satisfactory outcomes at stopping time.

On some tasks (Branin, Hartmann-3 and Rosenbrock-4), models were sufficiently well-calibrated and model-based stopping rules generally performed well. On others (GP-4 and Hartmann-6), overconfident models caused optimization runs or model-based stopping to miss the mark. For 4D functions drawn from GP priors, the variance of f was often underestimated. For Hartmann-6, the smoothness of f was often overestimated. It is worth mentioning that 33% of the underlying optimization runs on Hartmann-6 converged to a local minimum valued at -3.20 rather than the global minimum of -3.32 (see Table 12). Hence, each of these runs and the vast majority of stopping rule experiments would have succeeded if $\epsilon = 0.1$ was slightly larger.

These results highlight the importance of uncertainty calibration. Our hyperpriors were chosen to avoid strong inductive biases and this flexibility increased the chances of errant model fits. In practice, we suggest using conservative priors that favor smaller lengthscales and larger variances. Calibration may also be improved by marginalizing over hyperparameters (Simpson et al., 2021) or utilizing more expressive models, such as deep GPs (Salimbeni & Deisenroth, 2017) or Bayesian neural networks (Li et al., 2023). Note that while our analysis is specific to GPs, PRB only assumes that we can sample ϵ -optimality indicators.

7. Discussion

To the best of our knowledge, results presented here are among the first of their kind for Bayesian optimization. Supposing the prior distribution of problems is known, we have shown that the proposed stopping criterion (PRB) guarantees BO will return a solution that the user finds satisfactory with high probability. Further, we have demonstrated empirically that these findings carry over in practice for well-calibrated models.

Nevertheless, there is still more work to be done. These same empirical results echo initial skepticism about placing too much faith in our models. The success of the proposed stopping rule (and others like it) will depend in large part on our ability to overcome this challenge. To the extent that models prove trustworthy however, we suggest that model-based stopping may one day become as common place as model-based optimization.

Impact Statement

The goal of this work is to introduce a model-based stopping rule for Bayesian optimization that saves resources and alleviates the burden on the user. As is usually the case, automating real-world decisions comes with a certain degree of risk. Still, we remain optimistic that our work will have a positive impact on theoretical and applied fronts.

References

- Abadi, M., Agarwal, A., Barham, P., Brevdo, E., Chen, Z., Citro, C., Corrado, G. S., Davis, A., Dean, J., Devin, M., Ghemawat, S., Goodfellow, I., Harp, A., Irving, G., Isard, M., Jia, Y., Jozefowicz, R., Kaiser, L., Kudlur, M., Levenberg, J., Mané, D., Monga, R., Moore, S., Murray, D., Olah, C., Schuster, M., Shlens, J., Steiner, B., Sutskever, I., Talwar, K., Tucker, P., Vanhoucke, V., Vasudevan, V., Viégas, F., Vinyals, O., Warden, P., Wattenberg, M., Wicke, M., Yu, Y., and Zheng, X. TensorFlow: Large-scale machine learning on heterogeneous systems, 2015. URL <https://www.tensorflow.org/>. Software available from tensorflow.org.
- Adler, R. J. and Taylor, J. E. *Random fields and geometry*. Springer Science & Business Media, 2009.
- Audibert, J.-Y., Munos, R., and Szepesvári, C. Tuning bandit algorithms in stochastic environments. In *International conference on algorithmic learning theory*, pp. 150–165. Springer, 2007.
- Balandat, M., Karrer, B., Jiang, D. R., Daulton, S., Letham, B., Wilson, A. G., and Bakshy, E. BoTorch: A Framework for Efficient Monte-Carlo Bayesian Optimization. In *Advances in Neural Information Processing Systems* 33, 2020. URL <http://arxiv.org/abs/1910.06403>.
- Bardenet, R., Doucet, A., and Holmes, C. Towards scaling up Markov chain Monte Carlo: an adaptive subsampling approach. In *International conference on machine learning*, pp. 405–413. PMLR, 2014.
- Bishop, C. Pattern recognition and machine learning. *Springer google schola*, 2:531–537, 2006.
- Borell, C. The Brunn-Minkowski inequality in Gauss space. *Inventiones mathematicae*, 30(2):207–216, 1975.
- Byrd, R. H., Lu, P., Nocedal, J., and Zhu, C. A limited memory algorithm for bound constrained optimization. *SIAM Journal on scientific computing*, 16(5):1190–1208, 1995.
- Cai, X., Gomes, S., and Scarlett, J. Lenient regret and good-action identification in Gaussian process bandits. In *International Conference on Machine Learning*, pp. 1183–1192. PMLR, 2021.
- Frazier, P., Powell, W., and Dayanik, S. The knowledge-gradient policy for correlated normal beliefs. *INFORMS journal on Computing*, 21(4):599–613, 2009.
- Garnett, R. *Bayesian optimization*. Cambridge University Press, 2023.
- Griffiths, R.-R. and Hernández-Lobato, J. M. Constrained Bayesian optimization for automatic chemical design using variational autoencoders. *Chemical science*, 11(2): 577–586, 2020.
- Grünewälder, S., Audibert, J.-Y., Opper, M., and Shawe-Taylor, J. Regret bounds for Gaussian process bandit problems. In *Proceedings of the thirteenth international conference on artificial intelligence and statistics*, pp. 273–280. JMLR Workshop and Conference Proceedings, 2010.
- Hansen, N. The CMA evolution strategy: A tutorial. *arXiv preprint arXiv:1604.00772*, 2016.
- Jones, D. R. A taxonomy of global optimization methods based on response surfaces. *Journal of global optimization*, 21:345–383, 2001.
- Kushner, H. J. A versatile stochastic model of a function of unknown and time varying form. *Journal of Mathematical Analysis and Applications*, 5(1):150–167, 1962.
- Lederer, A., Umlauft, J., and Hirche, S. Posterior variance analysis of Gaussian processes with application to average learning curves. *arXiv preprint arXiv:1906.01404*, 2019a.

- Lederer, A., Umlauft, J., and Hirche, S. Uniform error bounds for Gaussian process regression with application to safe control. *Advances in Neural Information Processing Systems*, 32, 2019b.
- Li, Y. L., Rudner, T. G., and Wilson, A. G. A study of Bayesian neural network surrogates for Bayesian optimization. *arXiv preprint arXiv:2305.20028*, 2023.
- Makarova, A., Shen, H., Perrone, V., Klein, A., Faddoul, J. B., Krause, A., Seeger, M., and Archambeau, C. Automatic termination for hyperparameter optimization. In *International Conference on Automated Machine Learning*, pp. 7–1. PMLR, 2022.
- Massart, P. *Concentration inequalities and model selection: Ecole d’Eté de Probabilités de Saint-Flour XXXIII-2003*. Springer, 2007.
- Matthews, A. G. d. G., van der Wilk, M., Nickson, T., Fujii, K., Boukouvalas, A., León-Villagrà, P., Ghahramani, Z., and Hensman, J. GPflow: A Gaussian process library using TensorFlow. *Journal of Machine Learning Research*, 18(40):1–6, apr 2017. URL <http://jmlr.org/papers/v18/16-537.html>.
- Maurer, A. and Pontil, M. Empirical Bernstein bounds and sample variance penalization. *arXiv preprint arXiv:0907.3740*, 2009.
- Mnih, V., Szepesvári, C., and Audibert, J.-Y. Empirical Bernstein stopping. In *Proceedings of the 25th international conference on Machine learning*, pp. 672–679, 2008.
- Moćkus, J. On Bayesian methods for seeking the extremum. In *Optimization Techniques IFIP Technical Conference: Novosibirsk, July 1–7, 1974*, pp. 400–404. Springer, 1975.
- Nguyen, V., Gupta, S., Rana, S., Li, C., and Venkatesh, S. Regret for expected improvement over the best-observed value and stopping condition. In *Asian conference on machine learning*, pp. 279–294. PMLR, 2017.
- Picheny, V., Berkeley, J., Moss, H. B., Stojic, H., Granta, U., Ober, S. W., Artemev, A., Ghani, K., Goodall, A., Paleyes, A., Vakili, S., Pascual-Diaz, S., Markou, S., Qing, J., Loka, N. R. B. S., and Couckuyt, I. Trieste: Efficiently exploring the depths of black-box functions with tensorflow, 2023. URL <https://arxiv.org/abs/2302.08436>.
- Rahimi, A. and Recht, B. Random features for large-scale kernel machines. *Advances in neural information processing systems*, 20, 2007.
- Salimbeni, H. and Deisenroth, M. Doubly stochastic variational inference for deep Gaussian processes. *Advances in neural information processing systems*, 30, 2017.
- Šaltenis, V. R. On a method of multi-extremal optimization. *Automatics and Computers (Avtomatika i Vychislitel'nayya Tekhnika)*, 3:33–38, 1971.
- Scott, W., Frazier, P., and Powell, W. The correlated knowledge gradient for simulation optimization of continuous parameters using Gaussian process regression. *SIAM Journal on Optimization*, 21(3):996–1026, 2011.
- Simon, H. A. Rational choice and the structure of the environment. *Psychological review*, 63(2):129, 1956.
- Simpson, F., Lalchand, V., and Rasmussen, C. E. Marginalised Gaussian processes with nested sampling. *Advances in neural information processing systems*, 34: 13613–13625, 2021.
- Snoek, J., Larochelle, H., and Adams, R. P. Practical Bayesian optimization of machine learning algorithms. *Advances in neural information processing systems*, 25, 2012.
- Srinivas, N., Krause, A., Kakade, S. M., and Seeger, M. Gaussian process optimization in the bandit setting: No regret and experimental design. *arXiv preprint arXiv:0912.3995*, 2009.
- Sutton, R. S. and Barto, A. G. *Reinforcement learning: An introduction*. MIT press, 2018.
- Törn, A. and Žilinskas, A. *Global optimization*, volume 350. Springer, 1989.
- Tsirelson, B., Ibragimov, I., and Sudakov, V. Norms of Gaussian sample functions. In *Proceedings of the Third Japan—USSR Symposium on Probability Theory*, volume 550, pp. 20–41. Tashkent, 1976.
- Vazquez, E. and Bect, J. Convergence properties of the expected improvement algorithm with fixed mean and covariance functions. *Journal of Statistical Planning and inference*, 140(11):3088–3095, 2010.
- von Kügelgen, J., Rubenstein, P. K., Schölkopf, B., and Weller, A. Optimal experimental design via Bayesian optimization: active causal structure learning for Gaussian process networks. *arXiv preprint arXiv:1910.03962*, 2019.
- Wilson, J., Hutter, F., and Deisenroth, M. Maximizing acquisition functions for Bayesian optimization. *Advances in neural information processing systems*, 31, 2018.

Wilson, J., Borovitskiy, V., Terenin, A., Mostowsky, P., and Deisenroth, M. Efficiently sampling functions from Gaussian process posteriors. In *International Conference on Machine Learning*, pp. 10292–10302. PMLR, 2020.

Wilson, J. T., Borovitskiy, V., Terenin, A., Mostowsky, P., and Deisenroth, M. P. Pathwise conditioning of Gaussian processes. *The Journal of Machine Learning Research*, 22(1):4741–4787, 2021.

A. Technical proofs

Findings presented in the body of this paper rely upon a number of supporting results, some of which borrow heavily from earlier works. The main results of this section are as follows. Lemma 5 shows that the posterior variance becomes arbitrarily small as \mathbf{X}_t becomes increasingly dense in \mathcal{X} . Lemma 7 upper bounds the expected supremum of $f \sim \mathcal{GP}(0, k)$ based on its maximum variance. Theorem 2 and Corollary 8 prove that the PRB stopping criterion (5) almost surely converges. Finally, Theorem 3 shows that Bayesian optimization using PRB terminates and returns an (ϵ, δ) -optimal solution.

Where relevant, we will attribute credit at the beginning of the corresponding proof.

Proposition 4. *Let $\mathcal{X} \subseteq \mathbb{R}^D$ be convex and suppose that $\mathbf{X} \subseteq \mathcal{X}$ generates an ϵ -cover of \mathcal{X} . For every $\mathbf{x} \in \mathcal{X}$ and $\rho \geq \epsilon$, the intersection of the set \mathbf{X} and the ball $B(\mathbf{x}, \rho) = \{\mathbf{x}' \in \mathcal{X} : \|\mathbf{x} - \mathbf{x}'\|_\infty \leq \rho\}$ generates a 2ϵ -cover of $B(\mathbf{x}, \rho)$.*

Proof. Consider the ball $B(\mathbf{x}, r)$ with radius $r = \rho - \epsilon$. Since \mathcal{X} is convex, for every point $\mathbf{a} \in B(\mathbf{x}, \rho)$ there exists a $\mathbf{b} \in B(\mathbf{x}, r)$ such that $\|\mathbf{a} - \mathbf{b}\|_\infty \leq \epsilon$. Moreover, because \mathbf{X} generates an ϵ -cover of \mathcal{X} , for every point $\mathbf{b} \in B(\mathbf{x}, r)$ there exists a $\mathbf{c} \in \mathbf{X}$ so that $\|\mathbf{b} - \mathbf{c}\|_\infty \leq \epsilon$, which implies that $\mathbf{c} \in B(\mathbf{x}, \rho)$. It follows by the triangle inequality that for every point $\mathbf{a} \in B(\mathbf{x}, \rho)$ there exists a pair of points $\mathbf{b}, \mathbf{c} \in B(\mathbf{x}, r) \times [B(\mathbf{x}, \rho) \cap \mathbf{X}]$ such that

$$\|\mathbf{a} - \mathbf{c}\|_\infty \leq \|\mathbf{a} - \mathbf{b}\|_\infty + \|\mathbf{b} - \mathbf{c}\|_\infty \leq \epsilon + \epsilon = 2\epsilon, \quad (18)$$

which completes the proof. \square

Lemma 5. *Under assumptions A1 and A2, if $y(\cdot) \sim \mathcal{N}(f(\cdot), \gamma^2)$ is observed on a set of points $\mathbf{X} \subseteq \mathcal{X}$ that generates an ϵ -cover of \mathcal{X} , $0 \leq \epsilon \leq \min\{1, k(\mathbf{x}, \mathbf{x})/L_k\}$, then*

$$\text{Var}[f(\mathbf{x}) \mid y(\mathbf{X})] \leq \kappa_\epsilon(\mathbf{x}), \quad (19)$$

where

$$\kappa_\epsilon(\mathbf{x}) = \frac{[4L_k\rho(\epsilon)k(\mathbf{x}, \mathbf{x}) - L_k^2\rho(\epsilon)^2]\eta(\epsilon) + \gamma^2k(\mathbf{x}, \mathbf{x})}{[k(\mathbf{x}, \mathbf{x}) + 2L_k\rho(\epsilon)]\eta(\epsilon) + \gamma^2}$$

is given in terms of $\eta(\epsilon) = \max\{1, \rho(\epsilon)/4\epsilon\}^D$ and $\rho(\epsilon) = \epsilon^\epsilon$ for any $0 < \epsilon < 1$.

Proof. This result extends Lederer et al. (2019a, Theorem 3.1), who showed that, for all $0 \leq \rho \leq k(\mathbf{x}, \mathbf{x})/L_k$,

$$\text{Var}[f(\mathbf{x}) \mid y(\mathbf{B}_\rho(\mathbf{x}))] \leq \frac{(4L_k\rho k(\mathbf{x}, \mathbf{x}) - L_k^2\rho^2)|\mathbf{B}_\rho(\mathbf{x})| + \gamma^2k(\mathbf{x}, \mathbf{x})}{(k(\mathbf{x}, \mathbf{x}) + 2L_k\rho)|\mathbf{B}_\rho(\mathbf{x})| + \gamma^2} \quad \mathbf{B}_\rho(\mathbf{x}) = B(\mathbf{x}, \rho) \cap \mathbf{X}. \quad (20)$$

We would like to translate this upper bound as a function of $0 \leq \epsilon \leq 1$. To this end, begin by noticing that the upper bound in (20) increases monotonically on $0 \leq \rho \leq k(\mathbf{x}, \mathbf{x})/L_k$ and decreases monotonically on $n = |\mathbf{B}_\rho(\mathbf{x})| \in \mathbb{W}$. Substituting $\rho(\epsilon)$ for ρ and $\eta(\epsilon)$ for n therefore yields a valid bound so long as $\rho \leq \rho(\epsilon) \leq k(\mathbf{x}, \mathbf{x})/L_k$ and $0 \leq \eta(\epsilon) \leq n$. As in (20), $\rho(\epsilon)$ defines the radius of a ball around \mathbf{x} and $\eta(\epsilon)$ conveys the number of elements from \mathbf{X} that lie within this ball.

Starting with the latter, lower bounds on the cardinality of $\mathbf{B}_\rho(\mathbf{x})$ may be obtained from the fact that \mathbf{X} is assumed to generate an ϵ -cover of \mathcal{X} . By Proposition 4, it follows that $\mathbf{B}_\rho(\mathbf{x})$ generates a 2ϵ -cover of $B(\mathbf{x}, \rho)$. Accordingly, $|\mathbf{B}_\rho(\mathbf{x})|$ must be greater-equal to the minimum number of points required to construct such a cover. Under the $\|\cdot\|_\infty$ norm, the ϵ -covering number of a ball

$$B(\mathbf{x}, \rho) = \prod_{d=1}^D [\max(x_d - \rho, 0), \min(x_d + \rho, 1)] \quad (21)$$

is given by

$$M(B(\mathbf{x}, \rho), \|\cdot\|_\infty, \epsilon) = \prod_{d=1}^D \left\lceil \frac{\min(x_d + \rho, 1) - \max(0, x_d - \rho)}{2\epsilon} \right\rceil. \quad (22)$$

This number is minimized when $B(\cdot, \rho)$ is placed in a corner, such as $B(\mathbf{0}, \rho) = [0, \rho]^D$. Choosing

$$\eta(\varepsilon) = 1 \vee \left\lceil \frac{\rho(\varepsilon)}{4\varepsilon} \right\rceil^D \leq \left\lceil \frac{\rho(\varepsilon)}{4\varepsilon} \right\rceil^D \quad (23)$$

therefore ensures that $\eta(\varepsilon)$ lower bounds the cardinality of every $\mathbf{B}_\rho(\cdot)$. Note that there are two factors of two at play here: one accounts for the fact that $\mathbf{B}_\rho(\cdot)$ is only guaranteed to provide a 2ε -cover of $B(\cdot, \rho)$, and the other accounts for the fact that the corner balls are up to 2^D times smaller than other balls with the same radius.

Turning our attention to the choice of function $\rho(\varepsilon)$, some desiderata come into focus. First, we require $\rho(\varepsilon) \geq \varepsilon$ so that every $\mathbf{B}_\rho(\cdot)$ is nonempty. Second, we desire $\lim_{\varepsilon \rightarrow 0^+} \rho(\varepsilon) = 0$ because the resulting posterior variance bound will increase monotonically in $\rho(\varepsilon)$. Lastly, we want the ratio of $\rho(\varepsilon)$ to ε to diverge to infinity as ε approaches zero from above so that $\lim_{\varepsilon \rightarrow 0^+} \eta(\varepsilon) = \infty$. Based on these criteria, a convenient choice when $\mathcal{X} = [0, 1]^D$ is

$$\rho(\varepsilon) = \varepsilon^\alpha \quad 0 < \alpha < 1. \quad (24)$$

In summary, the claim follows by expressing ρ as a function of ε and using it to lower bound $|\mathbf{B}_\rho(\cdot)|$ with $\eta(\varepsilon)$:

$$\text{Var}[f(\mathbf{x}) \mid y(\mathbf{X})] \leq \frac{(4L_k\rho(\varepsilon)k(\mathbf{x}, \mathbf{x}) - L_k^2\rho(\varepsilon)^2)\eta(\varepsilon) + \gamma^2k(\mathbf{x}, \mathbf{x})}{(k(\mathbf{x}, \mathbf{x}) + 2L_k\rho(\varepsilon))\eta(\varepsilon) + \gamma^2}. \quad (25)$$

□

Proposition 6. For any choice of constants $a > 0$, $b \geq 0$, $c \geq 0$,

$$\int_0^c \sqrt{\log(1 + b\varepsilon^{-1/a})} d\varepsilon \leq c\sqrt{a^{-1} + \log(1 + bc^{-1/a})}. \quad (26)$$

Proof. The following proof originally appeared in Grünwalder et al. (2010, Appendix A). Let $\xi = (1 + \sqrt[a]{cb^{-1}})^a$ so that

$$\int_0^c \sqrt{\log(1 + b\varepsilon^{-1/a})} d\varepsilon \leq \int_0^c \sqrt{\log(\xi^{1/a}b\varepsilon^{-1/a})} d\varepsilon. \quad (27)$$

Next, define auxiliary functions

$$f(u) = \sqrt{\log(u^{-1/a})} \quad g(\varepsilon) = \frac{\varepsilon}{\xi b^a} \quad (28)$$

such that $f(g(\varepsilon)) = \sqrt{\log(\xi^{1/a}b\varepsilon^{-1/a})}$, and use them to integrate by substitution:

$$\int_0^c \sqrt{\log(\xi^{1/a}b\varepsilon^{-1/a})} d\varepsilon = \xi b^a \int_0^{g(c)} \sqrt{\log(u^{-1/a})} du = \frac{\xi b^a}{\sqrt{a}} \int_0^{g(c)} \sqrt{-\log(u)} du. \quad (29)$$

The Cauchy-Schwarz inequality now gives

$$\int_0^{g(c)} \sqrt{-\log(u)} du \leq \left(\int_0^{g(c)} du \right)^{1/2} \left(- \int_0^{g(c)} \log(u) du \right)^{1/2} = \frac{c}{\xi b^a} \sqrt{1 - \log\left(\frac{c}{\xi b^a}\right)}. \quad (30)$$

Hence, the claim follows

$$\int_0^c \sqrt{\log(1 + b\varepsilon^{-1/a})} d\varepsilon \leq c\sqrt{\frac{1 + \log(\xi b^a c^{-1})}{a}} = c\sqrt{a^{-1} + \log(1 + bc^{-1/a})}. \quad (31)$$

For comparison with Grünwalder et al. (2010), we have

$$b^a = 2c \implies \xi = \left(1 + 2^{-1/a}\right)^a \leq 2^a \implies c\sqrt{\frac{1 + \log(\xi b^a c^{-1})}{a}} = c\sqrt{\frac{1 + \log(2\xi)}{a}} \leq c\sqrt{\frac{\log(e2^{a+1})}{a}}. \quad (32)$$

□

Lemma 7. Let $f \sim \mathcal{GP}(0, k)$ be a Gaussian process with an L_k -Lipschitz continuous covariance function $k : \mathcal{X}^2 \rightarrow \mathbb{R}$ on $\mathcal{X} = [0, r]^D$ having maximum variance $\sigma^2 = \max_{\mathbf{x} \in \mathcal{X}} k(\mathbf{x}, \mathbf{x})$. Then,

$$\mathbb{E} \left[\sup_{\mathbf{x} \in \mathcal{X}} f(\mathbf{x}) \right] \leq 12\sigma \sqrt{2D + D \log(1 + 4L_k r \sigma^{-2})}. \quad (33)$$

Proof. This proof paraphrases parts of Grünewälder et al. (2010, Section 4.3).

Massart (2007, Theorem 3.18) proved that the expected supremum of f is upper bounded by

$$\mathbb{E} \left[\sup_{\mathbf{x} \in \mathcal{X}} f(\mathbf{x}) \right] \leq 12 \int_0^\sigma \sqrt{\log N(\mathcal{X}, d_k, \varepsilon)} d\varepsilon, \quad (34)$$

where $N(\mathcal{X}, d_k, \varepsilon)$ is defined as the ε -packing number—i.e. the largest number of points that can be “packed” inside of \mathcal{X} without any two points being within ε of one another—under the canonical pseudo-metric⁴

$$d_k(\mathbf{x}, \mathbf{x}') = \mathbb{E}[(f(\mathbf{x}) - f(\mathbf{x}'))^2]^{1/2} = \sqrt{k(\mathbf{x}, \mathbf{x}) - 2k(\mathbf{x}, \mathbf{x}') + k(\mathbf{x}', \mathbf{x}')}. \quad (35)$$

We may use (34) by upper bounding the right-hand side with a known quantity. We will bound the ε -packing number $N(\mathcal{X}, d_k, \varepsilon)$, translate this bound from the d_k pseudo-metric to the infinity norm, and then integrate the result.

The first step follows immediately from the fact that the ε -packing number is smaller than the $\frac{\varepsilon}{2}$ -covering number—defined as the minimum number of balls $B(\cdot, \frac{\varepsilon}{2})$ required to cover \mathcal{X} . The second is accomplished by using Lipschitz continuity of k to show that the squared pseudo-metric $d_k(\cdot, \cdot)^2$ is $2L_k$ -Lipschitz:

$$d_k(\mathbf{x}, \mathbf{x}')^2 = [k(\mathbf{x}, \mathbf{x}) - k(\mathbf{x}, \mathbf{x}')] + [k(\mathbf{x}', \mathbf{x}') - k(\mathbf{x}', \mathbf{x})] \leq 2L_k \|\mathbf{x} - \mathbf{x}'\|_\infty \quad \forall \mathbf{x}, \mathbf{x}' \in \mathcal{X}. \quad (36)$$

Given a set $\mathbf{X} \subseteq \mathcal{X}$ such that $\max_{\mathbf{x} \in \mathcal{X}} \min_{\mathbf{x}' \in \mathbf{X}} \|\mathbf{x} - \mathbf{x}'\|_\infty \leq C$, it follows that $\max_{\mathbf{x} \in \mathcal{X}} \min_{\mathbf{x}' \in \mathbf{X}} d_k(\mathbf{x}, \mathbf{x}') \leq \sqrt{2L_k C}$. An $\varepsilon^2/8L_k$ -cover under the infinity norm therefore guarantees an $\varepsilon/2$ -cover under d_k . The former may be constructed from a grid of uniformly spaced points with elements at intervals of $\varepsilon^2/4L_k$. Such a grid will consist of $\lceil 4L_k r \varepsilon^{-2} \rceil^D$ points assuming $\mathcal{X} = [0, r]^D$, meaning that

$$N(\mathcal{X}, d_k, \varepsilon) < (1 + 4L_k r \varepsilon^{-2})^D. \quad (37)$$

To complete the proof, use Proposition 6 with $a = \frac{1}{2}$, $b = 4L_k r$, and $c = \sigma$ to show that

$$\mathbb{E} \left[\sup_{\mathbf{x} \in \mathcal{X}} f(\mathbf{x}) \right] \leq 12\sqrt{D} \int_0^\sigma \sqrt{\log(1 + 4L_k r \varepsilon^{-2})} d\varepsilon \leq 12\sigma \sqrt{2D + D \log(1 + 4L_k r \sigma^{-2})}. \quad (38)$$

□

Theorem 2. Under assumptions A1–A3 and for all regret bounds $\epsilon > 0$ and risk tolerances $\delta > 0$, there almost surely exists a $T \in \mathbb{N}$ so that, at every time $t \geq T$, each point $\mathbf{s}_t \in \arg \max_{\mathbf{x} \in \mathcal{X}} \mu_t(\mathbf{x})$ satisfies

$$\mathbb{P} \left[\sup_{\mathbf{x} \in \mathcal{X}} f_t(\mathbf{x}) - f_t(\mathbf{s}_t) \leq \epsilon \right] \geq 1 - \delta. \quad (14)$$

Proof. Consider the centered process

$$g_t(\cdot) = [f_t(\cdot) - \mu_t(\cdot)] - [f_t(\mathbf{s}_t) - \mu_t(\mathbf{s}_t)], \quad (39)$$

with covariance

$$c_t(\mathbf{x}, \mathbf{x}') = k_t(\mathbf{x}, \mathbf{x}') - k_t(\mathbf{x}, \mathbf{s}_t) - k_t(\mathbf{s}_t, \mathbf{x}') + k_t(\mathbf{s}_t, \mathbf{s}_t). \quad (40)$$

The term $\mu_t(\mathbf{s}_t) - \mu_t(\cdot)$ is nonnegative by construction such that

$$g_t^* = \sup_{\mathbf{x} \in \mathcal{X}} g_t(\mathbf{x}) \geq f_t^* - f_t(\mathbf{s}_t) \quad f_t^* = \sup_{\mathbf{x} \in \mathcal{X}} f_t(\mathbf{x}) \quad (41)$$

⁴While d_k has most of the properties of a proper metric, $d_k(\mathbf{x}, \mathbf{x}') = 0$ does not always imply that $\mathbf{x} = \mathbf{x}'$ (Adler & Taylor, 2009).

and, therefore,

$$\mathbb{P}(g_t^* \geq \epsilon) \geq \mathbb{P}(f_t^* - f_t(\mathbf{s}_t) \geq \epsilon). \quad (42)$$

We would now like to use the Borell-TIS inequality (Borell, 1975; Tsirelson et al., 1976) to show that: if $\epsilon > \mathbb{E}(g_t^*)$, then

$$\mathbb{P}(g_t^* \geq \epsilon) \leq \exp\left(-\frac{1}{2} \left[\frac{\epsilon - \mathbb{E}(g_t^*)}{2\sigma_t}\right]^2\right), \quad (43)$$

where $\sigma_t = \max_{\mathbf{x} \in \mathcal{X}} \sqrt{k_t(\mathbf{x}, \mathbf{x})}$ and $2\sigma_t$ appears in the denominator (rather than σ_t) because $\max_{\mathbf{x} \in \mathcal{X}} c_t(\mathbf{x}, \mathbf{x}) \leq 4\sigma_t^2$. Since (43) is an increasing, continuous function of both $\sigma_t \geq 0$ and $0 \leq \mathbb{E}(g_t^*) < \epsilon$, the claim will hold if these quantities vanish as the (global) fill distance $h_t = \max_{\mathbf{x} \in \mathcal{X}} \min_{1 \leq i \leq t} \|\mathbf{x} - \mathbf{x}_i\|_\infty$ goes to zero.

The former result is an immediate consequence of Lemma 5. Regarding the latter, $f_t(\mathbf{s}_t) - \mu_t(\mathbf{s}_t)$ is a centered random variable. It follows by linearity of expectation that

$$\mathbb{E}(g_t^*) = \mathbb{E}\left[\sup_{\mathbf{x} \in \mathcal{X}} f_t(\mathbf{x}) - \mu_t(\mathbf{x})\right]. \quad (44)$$

Next, denote the canonical pseudo-metric at time t by

$$d_{k_t}(\mathbf{x}, \mathbf{x}') = \mathbb{E}[(f_t(\mathbf{x}) - f_t(\mathbf{x}'))^2]^{1/2} = \sqrt{k_t(\mathbf{x}, \mathbf{x}) - 2k_t(\mathbf{x}, \mathbf{x}') + k_t(\mathbf{x}', \mathbf{x}')}. \quad (45)$$

This pseudo-metric is non-increasing in t . To see this, let $\beta = k(\mathbf{x}_{t+1}, \mathbf{x}) - k(\mathbf{x}_{t+1}, \mathbf{x}')$ and write

$$\begin{aligned} d_{k_{t+1}}(\mathbf{x}, \mathbf{x}')^2 &= k_{t+1}(\mathbf{x}, \mathbf{x}) - 2k_{t+1}(\mathbf{x}, \mathbf{x}') + k_{t+1}(\mathbf{x}', \mathbf{x}') \\ &= \underbrace{k_t(\mathbf{x}, \mathbf{x}) - 2k_t(\mathbf{x}, \mathbf{x}') + k_t(\mathbf{x}', \mathbf{x}')}_{d_{k_t}(\mathbf{x}, \mathbf{x}')^2} - \underbrace{\beta^2 [k_t(\mathbf{x}_{t+1}, \mathbf{x}_{t+1}) + \gamma^2]^{-1}}_{\geq 0}. \end{aligned} \quad (46)$$

As t increases, points therefore become closer together under the d_{k_t} pseudo-metric. For this reason, the posterior ϵ -packing number $N(\mathcal{X}, d_{k_t}, \epsilon)$ is less-equal to the prior ϵ -packing number $N(\mathcal{X}, d_k, \epsilon)$. Applying Lemma 7, we now have

$$\mathbb{E}(g_t^*) \leq \int_0^{\sigma_t} \sqrt{\log N(\mathcal{X}, d_{k_t}, \epsilon)} d\epsilon \leq \int_0^{\sigma_t} \sqrt{\log N(\mathcal{X}, d_k, \epsilon)} d\epsilon \leq 12\sigma_t \sqrt{2D + D \log(1 + 4L_k \sigma_t^{-2})}. \quad (47)$$

From here, note that (47) is an increasing, continuous function of σ_t that vanishes as $\sigma_t \rightarrow \infty$. By Lemma 5, the same is true of σ_t as a function of h_t . As a result, (43) becomes arbitrarily small as $h_t \rightarrow 0$ and there exists a constant $h_* > 0$ such that this upper bound is less-equal to δ whenever $h_t \leq h_*$. Finally, since (\mathbf{x}_t) is almost surely dense in \mathcal{X} , there almost surely exists a time $T \in \mathbb{N}$ such that

$$t \geq T \implies h_t \leq h_* \implies \mathbb{P}(g_t^* > \epsilon) \leq \delta \implies \mathbb{P}(f_t^* - f_t(\mathbf{s}_t) > \epsilon) \leq \delta. \quad (48)$$

□

Corollary 8. *Suppose assumptions A1–A3 hold and that there exists a constant $\epsilon' > 0$ so that, with probability one,*

$$\limsup_{t \rightarrow \infty} \left[\max_{\mathbf{x} \in \mathcal{X}} \mu_t(\mathbf{x}) - \mu_t(\mathbf{s}_t) \right] \leq \epsilon', \quad (49)$$

where $\mathbf{s}_t \in \arg \max_{\mathbf{x} \in \mathbf{X}_t} \mu_t(\mathbf{x})$. Then, for every $\epsilon > \epsilon'$ and $\delta \in (0, 1]$, there almost surely exists a time $T \in \mathbb{N}$ such that, for all $t \geq T$,

$$\mathbb{P}\left[\sup_{\mathbf{x} \in \mathcal{X}} f_t(\mathbf{x}) - f_t(\mathbf{s}_t) \leq \epsilon\right] \geq 1 - \delta. \quad (50)$$

Proof. Per (49), there almost surely exists an $S \in \mathbb{N}$ such that $t \geq S \implies \max_{\mathbf{x} \in \mathcal{X}} \mu_t(\mathbf{x}) - \mu_t(\mathbf{s}_t) \leq \epsilon'$. Theorem 2 therefore implies there almost surely exists a $T \geq S$ so that

$$t \geq T \implies \mathbb{P}[f_t^* - f_t(\mathbf{s}_t) \geq \epsilon - \epsilon'] \leq \delta, \quad (51)$$

which completes the proof. □

The assumption that the posterior mean approaches its maximum on (\mathbf{x}_t) protects against adversarial cases where—no matter how densely we observe f —there is always an $\mathbf{x} \in \mathcal{X} \setminus \mathbf{X}_t$ whose expected value $\mu_t(\mathbf{x})$ exceeds $\mu_t(\mathbf{s}_t)$ by at least ϵ . Note that (49) becomes a necessary condition when $\delta < \frac{1}{2}$. Nevertheless, it is unclear how to ensure this condition without making stronger assumptions for f and (\mathbf{x}_t) . One can use A2 and the Cauchy-Schwarz inequality to show that the posterior mean is Lipschitz continuous (Lederer et al., 2019b); but, its Lipschitz constant may continue to grow as $t \rightarrow \infty$, so (49) may not hold.

Theorem 3. *Given a regret bound $\epsilon > 0$ and risk tolerance $\delta > 0$, let $\Psi_t(\mathbf{s}_t)$ be the probability under the model at time $t \in \mathbb{N}$ that $\mathbf{s}_t \in \arg \max_{\mathbf{x} \in \mathcal{X}} \mu_t(\mathbf{x})$ is ϵ -optimal. Suppose that at each step t (or a subsequence thereof) an independent run of Algorithm 1 is used to produce a random, unbiased estimate $\Psi_t^n(\mathbf{s}_t)$ that is closer to $\Psi_t(\mathbf{s}_t)$ than it is to $1 - \delta_{\text{mod}}$ with probability at least $1 - \delta_{\text{est}}^t$, where δ_{mod} and δ_{est} are nonzero probabilities so that $\delta_{\text{mod}} + \delta_{\text{est}} \leq \delta$ and (δ_{est}^t) is a positive sequence satisfying $\sum_{i=1}^{\infty} \delta_{\text{est}}^i \leq \delta_{\text{est}}$.*

If assumptions A1–A3 hold and the first \mathbf{s}_t for which $\Psi_t^n(\mathbf{s}_t) \geq 1 - \delta_{\text{mod}}$ is returned, then the algorithm almost surely finishes in finite time with an (ϵ, δ) -optimal solution.

Proof. Under assumptions A1–A3, Theorem 2 implies that there almost surely exists an $S \in \mathbb{N}$ so that, at all times $t \geq S$, \mathbf{s}_t is $(\epsilon, \delta_{\text{mod}})$ -optimal. Since this event occurs infinitely often with probability one and each estimate $\Psi_t^n(\mathbf{s}_t)$ is independent and unbiased, there almost surely exists a least $T \in \mathbb{N}$ such that $\Psi_T(\mathbf{s}_T) \geq 1 - \delta_{\text{mod}}$ and $\Psi_T^n(\mathbf{s}_T) \geq 1 - \delta_{\text{mod}}$.

By assumption, each event

$$\mathcal{A}_t = \{|\Psi_t^n(\mathbf{s}_t) - \Psi_t(\mathbf{s}_t)| \leq |\Psi_t^n(\mathbf{s}_t) - \lambda|\} \quad t = 1, 2, \dots \quad (52)$$

occurs with probability at least $1 - \delta_{\text{est}}^t$. If \mathcal{A}_t holds, then $\Psi_t^n(\mathbf{s}_t) \geq 1 - \delta_{\text{mod}}$ implies $\Psi_t(\mathbf{s}_t) \geq 1 - \delta_{\text{mod}}$. Per the union bound, the probability of terminating prior to T is therefore no larger than $\sum_{t=1}^{T-1} \delta_{\text{est}}^t \leq \delta_{\text{est}}$.

If the algorithm reaches T , then the probability that \mathbf{s}_T fails to be ϵ -optimal is less-equal to δ_{mod} by construction. Hence, the algorithm almost surely terminates and returns an ϵ -optimal solution with probability at least $1 - \delta_{\text{mod}} - \delta_{\text{est}} \geq 1 - \delta$. \square

B. Experiment Details

Implementation Code is available online at https://github.com/j-wilson/trieste_stopping. Experiments were run using a combination of GPFlow (Matthews et al., 2017) and Trieste (Picheny et al., 2023). Runtimes reported in Figure 3 were measured on an Apple M1 Pro Chip using an off-the-shelf version of TensorFlow (Abadi et al., 2015).

Model specification We employed Gaussian process priors $f \sim \mathcal{GP}(\mu, k)$ with constant mean functions $\mu(\cdot) = c$ and Matérn- $5/2$ covariance functions equipped with ARD lengthscales.

When optimizing functions drawn from GP priors, we set the prior mean to zero and used unit variance kernels with lengthscales $\ell_i = \frac{1}{4}\sqrt{D}$. Noise variances are indicated alongside reported results.

When optimizing black-box functions, we employed broad and uninformative hyperpriors. Let $[\mathcal{X}]_i = [a_i, b_i]$ be the range of the i -th design variable, $q_t : [0, 1] \rightarrow \mathbb{R}$ be the empirical quantile function of y at time t , and $\nu_t = \overline{\text{Var}}[\mathbf{y}_{t-1}]$ be the empirical variance of observations $\mathbf{y}_{t-1} = \{y(\mathbf{x}_1), \dots, y(\mathbf{x}_{t-1})\}$. Our hyperpriors are then as follows:

Name	Distribution	Parameters	
Constant Mean	Uniform(a, b)	$a = q_t(0.05)$	$b = q_t(0.95)$
Log Kernel Variance	Uniform(a, b)	$a = \log(10^{-1}\nu_t)$	$b = \log(10\nu_t)$
Log Noise Variance	Uniform(a, b)	$a = \log(10^{-9}\nu_t)$	$b = \log(10\nu_t)$
i -th Lengthscale	LogNormal(μ, σ)	$\mu = \frac{1}{2}(b_i - a_i)$	$\sigma = 1$

Note that we directly parameterize certain hyperparameters in log-space and that, e.g., $\log(\theta) \sim \text{Uniform}(a, b)$ is not the same as $\theta \sim \text{LogUniform}(e^a, e^b)$ (Bishop, 2006).

Acquisition function In our experiments, we defined the set of feasible solutions at time t as the set of evaluated points \mathbf{X}_t . Under these circumstances, one can show that the optimal one-step policy is given by an “in-sample” version of the Knowledge Gradient strategy (Moćkus, 1975; Frazier et al., 2009). Let

$$\mu_{t+1}(\cdot; \mathbf{x}, z) = \mu_t(\cdot) + \frac{k_t(\cdot, \mathbf{x})z}{\sqrt{k_t(\mathbf{x}, \mathbf{x}) + \gamma^2}} \quad (53)$$

be the posterior mean of f at time $t + 1$ if we observe $y_{t+1} = \mu_t(\mathbf{x}) + \sqrt{k_t(\mathbf{x}, \mathbf{x}) + \gamma^2}z$, where $z \sim \mathcal{N}(0, 1)$. Then, the aforementioned acquisition function is given by

$$\text{ISKG}_t(\mathbf{x}) = \mathbb{E}_z \left[\max \mu_{t+1}(\mathbf{X}_t \cup \{\mathbf{x}\}; \mathbf{x}, z) \right] - \max \mu_t(\mathbf{X}_t) \quad z \sim \mathcal{N}(0, 1). \quad (54)$$

ISKG is identical to the Expected Improvement function when $\gamma^2 = 0$ (Scott et al., 2011), but avoids pathologies (such as re-evaluated previously observed points) when $\gamma^2 > 0$.

In practice, we estimated (54) with Gauss-Hermite quadrature and maximized it using multi-start gradient ascent (Wilson et al., 2018; Balandat et al., 2020). Starting positions we obtained by running CMA-ES (Hansen, 2016) several times to partial convergence. The best point from each run was then combined with a large number of random points and the top 16 points were fine-tuned using L-BFGS-B (Byrd et al., 1995).

C. Extended Results

This section provides extended results for experiments presented in the body. Results are given for each problem in the order they appeared in Table 1. In each of the following table, we report success rates along with medians and interquartile ranges of stopping times, log regrets, and log excess regrets. Here, excess regret is defined as the amount by which regrets exceeded ϵ for runs that failed to return ϵ -optimal solutions, i.e. $\sup_{\mathbf{x} \in \mathcal{X}} f(\mathbf{x}) - f(\mathbf{s}_T) + \epsilon$. For compactness, table numbers and problems names are reported in the upper left corner.

2. GP-2*, 10^{-6}	ϵ -optimal	Stopping Time			Log ₁₀ Regret			Log ₁₀ Excess Regret		
Method	%	Q1	Q2	Q3	Q1	Q2	Q3	Q1	Q2	Q3
Oracle*	1.00	8	9	12	-5.88	-5.34	-4.81	–	–	–
Budget*	0.96	18	18	18	-4.25	-3.16	-2.21	-1.32	-0.98	-0.92
Budget	0.98	33	33	33	-4.99	-4.30	-3.78	-1.01	-0.99	-0.97
Acq. Cutoff*	0.99	23	26	33	-4.78	-4.25	-3.81	-1.03	-1.03	-1.03
UCB – LCB	0.89	10	12	15	-2.54	-2.00	-1.43	-1.00	-0.86	-0.21
PRB (ours)	0.97	14	17	21	-3.72	-2.96	-2.36	-1.30	-1.03	-0.94

3. GP-2*, 10^{-2}	ϵ -optimal	Stopping Time			Log ₁₀ Regret			Log ₁₀ Excess Regret		
Method	%	Q1	Q2	Q3	Q1	Q2	Q3	Q1	Q2	Q3
Oracle*	1.00	8	10	12	-4.35	-3.89	-3.20	–	–	–
Budget*	0.96	23	23	23	-2.49	-1.83	-1.42	-1.84	-1.66	-1.41
Budget	1.00	33	33	33	-2.91	-2.08	-1.60	–	–	–
Acq. Cutoff*	1.00	34.75	60.5	90.5	-3.08	-2.50	-2.20	–	–	–
UCB – LCB	1.00	70	82	99	-3.33	-2.77	-2.25	–	–	–
PRB (ours)	0.99	17	23	32	-2.51	-1.87	-1.58	-0.11	-0.11	-0.11

Stopping Bayesian Optimization with Probabilistic Regret Bounds

4. GP-4*, 10^{-6}		ϵ -optimal	Stopping Time			Log ₁₀ Regret			Log ₁₀ Excess Regret		
Method	%	Q1	Q2	Q3	Q1	Q2	Q3	Q1	Q2	Q3	
Oracle*	1.00	17.75	26	34	-4.24	-3.73	-3.33	–	–	–	
Budget*	0.95	65	65	65	-3.56	-3.11	-2.67	-1.70	-1.18	-0.62	
Budget	0.95	65	65	65	-3.56	-3.11	-2.67	-1.70	-1.18	-0.62	
Acq. Cutoff*	1.00	59.5	76.5	90	-3.66	-3.22	-2.93	–	–	–	
UCB – LCB	0.66	17.75	22.5	30	-1.98	-1.49	-0.81	-1.26	-0.70	-0.45	
PRB (ours)	0.99	46	64	78	-3.49	-3.10	-2.70	-2.67	-2.67	-2.67	

5. GP-4*, 10^{-2}		ϵ -optimal	Stopping Time			Log ₁₀ Regret			Log ₁₀ Excess Regret		
Method	%	Q1	Q2	Q3	Q1	Q2	Q3	Q1	Q2	Q3	
Oracle*	1.00	19	28.5	42	-2.66	-2.36	-1.92	–	–	–	
Budget*	0.95	95	95	95	-2.35	-1.82	-1.52	-1.63	-1.45	-1.30	
Budget	0.85	65	65	65	-1.94	-1.57	-1.22	-1.73	-1.35	-1.02	
Acq. Cutoff*	0.96	69.75	89	111	-2.24	-1.84	-1.53	-1.75	-1.47	-1.23	
UCB – LCB	1.00	223.75	256	256	-2.44	-1.97	-1.73	–	–	–	
PRB (ours)	0.96	67	86.5	113.25	-2.21	-1.81	-1.50	-1.92	-1.49	-1.14	

6. GP-4, 10^{-6}		ϵ -optimal	Stopping Time			Log ₁₀ Regret			Log ₁₀ Excess Regret		
Method	%	Q1	Q2	Q3	Q1	Q2	Q3	Q1	Q2	Q3	
Oracle*	1.00	21.5	34	50.5	-4.17	-3.66	-3.15	–	–	–	
Budget*	0.95	80	80	80	-3.59	-3.13	-2.58	-1.70	-1.47	-0.88	
Budget	0.85	65	65	65	-3.35	-2.88	-1.88	-1.11	-0.79	-0.55	
Acq. Cutoff*	0.97	61.75	77.5	91	-3.49	-3.15	-2.77	-1.58	-1.47	-1.43	
UCB – LCB	0.30	15	18	21.25	-1.25	-0.34	-0.08	-0.53	-0.25	-0.04	
PRB (ours)	0.88	48.25	61	75.25	-3.27	-2.85	-2.24	-1.41	-0.66	-0.49	

7. GP-4, 10^{-2}		ϵ -optimal	Stopping Time			Log ₁₀ Regret			Log ₁₀ Excess Regret		
Method	%	Q1	Q2	Q3	Q1	Q2	Q3	Q1	Q2	Q3	
Oracle*	1.00	29.75	50	74.75	-2.67	-2.32	-1.93	–	–	–	
Budget*	0.95	158	158	158	-2.24	-1.79	-1.51	-2.83	-1.39	-0.63	
Budget	0.61	65	65	65	-1.72	-1.30	-0.69	-1.26	-0.61	-0.31	
Acq. Cutoff*	0.96	88.75	112	142	-2.25	-1.75	-1.46	-2.08	-1.75	-1.68	
UCB – LCB	0.80	121.5	224	256	-2.30	-1.76	-1.19	-0.84	-0.31	-0.01	
PRB (ours)	0.92	73.75	100.5	129.5	-2.07	-1.69	-1.39	-1.78	-1.55	-1.31	

Stopping Bayesian Optimization with Probabilistic Regret Bounds

8. GP-6*, 10^{-6}		ϵ -optimal	Stopping Time			Log ₁₀ Regret			Log ₁₀ Excess Regret		
Method	%	Q1	Q2	Q3	Q1	Q2	Q3	Q1	Q2	Q3	
Oracle*	0.99	25	39.5	77.25	-3.71	-3.15	-2.69	-2.74	-2.74	-2.74	
Budget*	0.95	125	125	125	-3.04	-2.69	-2.26	-1.54	-1.16	-0.84	
Budget	0.86	97	97	97	-2.93	-2.42	-1.70	-1.51	-1.15	-0.74	
Acq. Cutoff*	0.97	86	115.5	153.5	-2.98	-2.60	-2.31	-2.05	-1.67	-1.26	
UCB – LCB	0.50	24	32.5	41.25	-1.63	-1.03	-0.47	-1.04	-0.62	-0.20	
PRB (ours)	0.98	97	133.5	178	-3.15	-2.77	-2.47	-2.47	-2.21	-1.94	

9. GP-6*, 10^{-2}		ϵ -optimal	Stopping Time			Log ₁₀ Regret			Log ₁₀ Excess Regret		
Method	%	Q1	Q2	Q3	Q1	Q2	Q3	Q1	Q2	Q3	
Oracle*	1.00	33	64	96.5	-2.41	-2.00	-1.72	–	–	–	
Budget*	0.96	228	228	228	-1.97	-1.70	-1.37	-1.73	-1.60	-1.39	
Budget	0.70	97	97	97	-1.53	-1.25	-0.87	-1.34	-0.98	-0.71	
Acq. Cutoff*	0.92	110.5	145	187.5	-1.76	-1.53	-1.30	-1.87	-1.56	-1.33	
UCB – LCB	1.00	499	512	512	-2.25	-1.91	-1.60	–	–	–	
PRB (ours)	1.00	170	235	295	-2.02	-1.76	-1.53	–	–	–	

10. Branin-2		ϵ -optimal	Stopping Time			Log ₁₀ Regret			Log ₁₀ Excess Regret		
Method	%	Q1	Q2	Q3	Q1	Q2	Q3	Q1	Q2	Q3	
Oracle*	1.00	13	18	21.25	-6.41	-6.34	-6.17	–	–	–	
Budget*	0.95	26	26	26	-2.79	-1.97	-1.45	-1.62	-1.54	-1.15	
Budget	1.00	33	33	33	-3.44	-3.02	-2.61	–	–	–	
Acq. Cutoff*	1.00	64	64	64	-6.23	-5.99	-5.69	–	–	–	
UCB – LCB	0.99	26.75	31	32	-3.08	-2.75	-2.38	0.16	0.16	0.16	
PRB (ours)	0.99	31	33	35	-3.44	-3.07	-2.72	0.16	0.16	0.16	

11. Hartmann-3		ϵ -optimal	Stopping Time			Log ₁₀ Regret			Log ₁₀ Excess Regret		
Method	%	Q1	Q2	Q3	Q1	Q2	Q3	Q1	Q2	Q3	
Oracle*	1.00	11	13	15.25	-6.66	-6.64	-6.58	–	–	–	
Budget*	0.96	23	23	23	-4.39	-3.81	-3.32	-0.80	-0.37	-0.18	
Budget	1.00	49	49	49	-6.58	-6.39	-6.05	–	–	–	
Acq. Cutoff*	1.00	23	25	27.25	-4.89	-4.50	-4.02	–	–	–	
UCB – LCB	0.83	14	15	16	-2.20	-1.98	-1.61	-0.17	-0.17	-0.17	
PRB (ours)	1.00	17	19	21	-3.81	-3.41	-2.90	–	–	–	

Stopping Bayesian Optimization with Probabilistic Regret Bounds

12. Hartmann-6	ϵ -optimal	Stopping Time			Log ₁₀ Regret			Log ₁₀ Excess Regret		
Method	%	Q1	Q2	Q3	Q1	Q2	Q3	Q1	Q2	Q3
Oracle*	0.67	25.75	35	256	-5.70	-5.69	-0.92	-1.72	-1.72	-1.72
Budget*	0.67	256	256	256	-5.70	-5.69	-0.92	-1.72	-1.72	-1.72
Budget	0.67	97	97	97	-5.66	-5.59	-0.92	-1.72	-1.72	-1.72
Acq. Cutoff*	0.67	35	38	42	-3.28	-2.81	-0.92	-1.71	-1.70	-1.68
UCB – LCB	0.46	18	26	31	-1.75	-0.85	0.03	-1.09	-0.59	0.47
PRB (ours)	0.64	37	40	43	-3.29	-2.82	-0.92	-1.71	-1.70	-1.67

13. Rosenbrock-4	ϵ -optimal	Stopping Time			Log ₁₀ Regret			Log ₁₀ Excess Regret		
Method	%	Q1	Q2	Q3	Q1	Q2	Q3	Q1	Q2	Q3
Oracle*	1.00	26	33	41	–	–	–	–	–	–
Budget*	0.95	47	47	47	-4.89	-4.53	-4.27	-5.35	-5.23	-4.60
Budget	1.00	65	65	65	-6.06	-5.68	-5.44	–	–	–
Acq. Cutoff*	0.94	60	62	64	-6.06	-5.59	-4.88	-4.40	-4.33	-4.26
UCB – LCB	1.00	71	73.5	76	–	–	–	–	–	–
PRB (ours)	1.00	81	84	88	–	–	–	–	–	–